

Surface-Electromagnetic-Wave-Enhanced Raman Scattering by Overlayers on Metals

Y. J. Chen,* W. P. Chen, and E. Burstein

*Department of Physics and the Laboratory for Research on the Structure of Matter,
University of Pennsylvania, † Philadelphia, Pennsylvania 19174*

(Received 18 March 1976)

Using a general formulation we show that by using surface electromagnetic waves in an attenuated-total-reflection prism configuration it should be possible to enhance the intensity of Raman scattering by a thin overlayer on a Ag surface by two orders of magnitude and that the use of surface electromagnetic waves may in fact make it possible to observe coherent anti-Stokes Raman scattering by the overlayer.

There is a continuing interest in the possibility of observing the Raman spectra of adsorbed layers on metal surfaces.^{1,2} Greenler and Slager¹ have recently reported the observation of well-defined, albeit weak, Raman scattering by a 50-Å overlayer of benzoic acid on an evaporated Ag film using the 4880-Å line of an argon-ion laser in an external-multiple-reflection scattering configuration. They suggest that, in the case of a strong scatterer such as benzoic acid, one should be able to observe the Raman spectrum of overlayers of the order of 10 Å in thickness. In this Letter we show that by using surface electromagnetic (SEM) waves as the incident and scattered electromagnetic radiation in an attenuated-total-reflection (ATR) prism scattering configuration it should be possible to enhance appreciably the intensity of Raman scattering by a thin overlayer on a metal over that in an external reflection (ER) scattering configuration. We show furthermore that, by using SEM waves, it may, in fact, be possible to observe coherent anti-Stokes Raman (CAR) scattering³ by the overlayer.

In an ATR prism configuration, and specifically the Kretschmann (prism-metal-film-vacuum) configuration,⁴ with an overlayer at the metal-vacuum interface, the dispersion curve of the SEM modes, which differs only slightly from that in the absence of the overlayer,⁵ has two branches. As one sweeps the angle of incidence, at fixed frequency, of a TM-polarized volume electromagnetic (VEM) wave in the prism one observes a minimum in the intensity of the reflected wave (R_{\min}), which is associated with a peak in the electromagnetic field (E_{\max}) in the overlayer,⁶ at an angle designated as $\theta_{\text{ATR}}(\omega)$. At this angle there is a strong linear coupling of the VEM wave with SEM modes of the upper branch of the dispersion curve which is associated with the metal-film-overlayer interface. When the overlayer is very thin $\theta_{\text{ATR}}(\omega)$, $R_{\min}(\omega)$, and $E_{\max}(\omega)$ do not differ appreciably from their values in the ab-

sence of the overlayer.⁵ The magnitude of $\theta_{\text{ATR}}(\omega)$, $R_{\min}(\omega)$, and $E_{\max}(\omega)$ depend on the thickness d and complex dielectric constant ($\tilde{\epsilon} = \epsilon' + i\epsilon''$) of the metal film. As shown by Otto,⁶ the largest E_{\max} and the smallest R_{\min} occur at an optimum thickness d_0 at which the "dielectric loss" in the metal and the "radiation loss" are equal.

In order to make a direct comparison of the Raman scattering by an adsorbed layer on a metal surface in the ER and in the ATR prism scattering configuration, we make use of a formulation which encompasses both scattering configurations. In the ER scattering configuration (Fig. 1) TM-polarized VEM radiation is incident at an angle θ_i , with respect to the normal to the metal surface, and scattered TM-polarized VEM radiation is collected at an angle θ_s (not necessarily collinear with θ_i), both angles being selected to yield a maximum scattering cross section. In the ATR prism scattering configuration, the "incident" SEM radiation is generated by linear coupling with TM-polarized VEM radiation in the prism propagating at an angle $\theta_i = \theta_{\text{ATR}}(\omega_i)$ and the scattered SEM radiation (not necessarily collinear with the incident SEM radiation) in turn generates TM-polarized VEM radiation in the prism, at an angle $\theta_s = \theta_{\text{ATR}}(\omega_s)$. It should be noted that when we refer to "incident" SEM radiation and "scattered" SEM radiation we are referring to EM modes which are predominately SEM mode in character. Such modes occur when VEM modes are incident at angle $\theta_i \simeq \theta_{\text{ATR}}(\omega_i)$ and are in turn detected when VEM waves are collected at $\theta_s \simeq \theta_{\text{ATR}}(\omega_s)$. One could have, of course, pure incident or scattered SEM modes in a two-prism configuration,⁷ but the latter is not practical at visible frequencies where the propagation length of the SEM waves is very small (microns).

The expression for the differential Raman scattering cross section of a thin overlayer on a metal surface, which is applicable to both the ER and ATR prism scattering configurations, can be

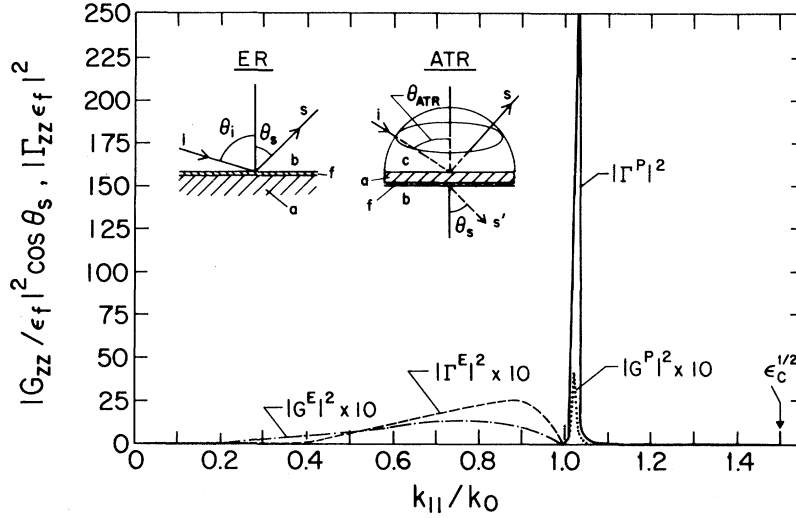


FIG. 1. Curves of $|\Gamma_{bfzz}^E \epsilon_f|^2$ and $|G_{fbzz}^E/\epsilon_f|^2 \cos \theta_s$ for the ER configuration and of $|\Gamma_{cfzz}^P \epsilon_f|^2 = |\Gamma_{cbzz}^P|^2$ and $|G_{fc\alpha x}^P/\epsilon_f|^2 \cos \theta_s = |G_{bc\alpha x}^P|^2 \cos \theta_s$ for the ATR prism configuration versus $k_{||}/k_0$ for a thin overlayer on silver, based on $\lambda_i \approx \lambda_s = 6471 \text{ \AA}$, $d_0 = 530 \text{ \AA}$, $\tilde{\epsilon}_{Ag} = -19.6 + i 0.59$, and $\epsilon_c = 2.25$.

readily shown to have the form⁸

$$\frac{d^2 I}{d\omega_s d\Omega} \propto \left(\frac{\omega_s}{c}\right)^4 \sum_{\alpha} \sum_{\beta \xi \nu} G_{\alpha\beta}(\omega_s, \vec{k}_{s||}) \delta \epsilon_{\beta\xi}(\omega_j, \vec{q}_{j||}) \Gamma_{\xi\nu}(\omega_i, \vec{k}_{i||}) |E_{i\nu}|^2 \mathfrak{D} \cos \theta_s,$$

where α, β, ξ, ν represents x, y, z with the normal to the metal film along z ; ω_i, ω_s , and $\omega_j = \omega_i - \omega_s$, and $\vec{k}_{i||}, \vec{k}_{s||}$, and $\vec{q}_{j||} = \vec{k}_{i||} - \vec{k}_{s||}$ are the frequencies and the components of the wave vector parallel to the surface of the incident radiation, scattered radiation, and vibration modes of the overlayer, respectively; $\delta \epsilon$ is the nonlinear dielectric tensor of the overlayer whose form determines the polarization selection rules; \underline{G} and $\underline{\Gamma}$ are the Fresnel transfer functions for the scattered and incident radiation, respectively; \mathfrak{D} is a kinematic "scattering length" which arises from integration over z and which is determined by the z dependence of the modes participating in the nonlinear interaction and by the thickness of the nonlinear medium; and only $\vec{k}_{||}$ is conserved in the scattering process. In the case of very thin adsorbed layers, with which we are concerned here, \mathfrak{D} reduces simply to Δl , the thickness of the layer. $\underline{\Gamma}$ relates the amplitudes of the electric field of the exciting radiation in the overlayer to the electric field \vec{E}_i of the incident VEM wave *either* in the vacuum in the case of ER configuration, *or* in the prism (medium c) in the case of ATR prism configuration. \underline{G} relates the electric field of the scattered VEM radiation, *either* in the vacuum in the ER configuration, *or* in the prism in the ATR configuration, to the electric field of the scattered radiation in the overlayer.

The components of the Fresnel transfer functions for TM radiation in the ATR prism configuration (Fig. 1) take relatively simple forms, as follows:

$$\Gamma_{cfzv}^P = E_{fx}^i/E_{cv}^i \approx \Gamma_{cbzv}^P; \quad \Gamma_{cfzv}^P = E_{fz}^i/E_{cv}^i \approx \Gamma_{cbzv}^P/\epsilon_f;$$

$$G_{fc\alpha x}^P = E_{c\alpha}^s/E_{fx}^s \approx G_{bc\alpha x}^P; \quad G_{fc\alpha x}^P = E_{cz}^s/E_{fz}^s \approx \epsilon_f G_{bc\alpha x}^P;$$

$$\Gamma_{cb\xi\nu}^P = \gamma_{\xi\nu}(\theta_i) \frac{T_{ca} T_{ab} \exp(ik_{az}^i d)}{1 - R_{ab} R_{ac} \exp(2ik_{az}^i d)} = \gamma_{\xi\nu}(\theta_i) \frac{4k_{az} k_{cz} \epsilon_a (\epsilon_b \epsilon_c)^{1/2} \exp(ik_{az}^i d)}{D};$$

$$G_{bc\alpha\beta}^P = g_{\alpha\beta}(\theta_s) \frac{T_{ba} T_{ac} \exp(ik_{az}^s d)}{1 - R_{ac} R_{ab} \exp(2ik_{az}^s d)} = g_{\alpha\beta}(\theta_s) \frac{4k_{az} k_{bz} \epsilon_a (\epsilon_b \epsilon_c)^{1/2} \exp(ik_{az}^s d)}{D};$$

$$D = (\epsilon_a k_{cz} + \epsilon_c k_{az})(\epsilon_b k_{az} + \epsilon_a k_{bz}) - (\epsilon_a k_{cz} - \epsilon_c k_{az})(\epsilon_b k_{az} - \epsilon_a k_{bz}) \exp(2ik_{az} d),$$

where the subscripts a , b , c , and f represent metal film, vacuum, prism, and overlayer, respectively; ϵ_a is the dielectric constant of the medium a , etc; $\tilde{k}_{az} = k_{az}' + ik_{az}'' = [\epsilon_a(\omega/c)^2 - k_{\parallel}^2]^{1/2}$ is the component of the wave vector of the EM waves normal to the interface in medium a ; $\Gamma_{cb}^{P_0}$ and $G_{cb}^{P_0}$ are Fresnel transfer functions in the absence of the overlayer, which relate the electric field of the incident and scattered radiation in medium b at the a - b interface to the corresponding fields in medium c ; $T_{ab} = 2k_{az}(\epsilon_a\epsilon_b)^{1/2}(\epsilon_a k_{bz} + \epsilon_b k_{az})$ and $R_{ab} = (\epsilon_b k_{az} - \epsilon_a k_{bz})/(\epsilon_b k_{az} + \epsilon_a k_{bz})$ are the Fresnel transmission and reflection coefficients, respectively, at the a - b interface, etc.; $\gamma_{\xi\nu}(\theta_i)$ and $g_{\alpha\beta}(\theta_s)$ are simple angular factors; and $D=0$ is the dispersion relation of the SEM modes in the ATR prism configuration.

At a given ω , $\Gamma_{cb}^{P_0}$ and $G_{bc}^{P_0}$ both exhibit peaks at $k_{\parallel}(\omega) = k_c \sin\theta_P(\omega)$ which lies very close to $k_{\parallel} = k_c \sin\theta_{\text{ATR}}(\omega)$.⁵ For metals such as Ag, with $\epsilon_a'' \ll |\epsilon_a'|$ in the visible, the thickness of the metal film d_0 at which $|\Gamma_{cb}^{P_0}(\theta_P)|^2$ and $|G_{bc}^{P_0}(\theta_P)|^2$ have their largest values, namely $d_0 = \ln|R_{ab} \times R_{ac}|_{\theta_P}/2k_{az}''$, is appreciably larger than the skin depth of the metal $\delta_{\text{EM}} = 1/2k_{az}''$.

The components of the Fresnel transfer functions for the ER scattering configuration take the following form:

$$\begin{aligned}\Gamma_{bfx\nu}^E &\simeq (1 - R_{ba})\gamma_{x\nu}(\theta_i); \\ \Gamma_{bfx\nu}^E &\simeq (1 + R_{ba})\gamma_{z\nu}(\theta_i)/\epsilon_f; \\ G_{fb\alpha x}^E &\simeq (1 - R_{ba})g_{\alpha x}(\theta_s); \\ G_{fb\alpha z}^E &\simeq \epsilon_f(1 + R_{ba})g_{\alpha z}(\theta_s).\end{aligned}$$

Curves giving the dependence of $|\epsilon_f\Gamma_{zz}|^2$ and $|G_{zz}/\epsilon_f|^2 \cos\theta_s$ on k_{\parallel} at $\lambda_i \simeq \lambda_s = 6471 \text{ \AA}$ for an ER configuration and for an ATR prism configuration involving a thin overlayer on Ag are shown in Fig. 1.⁹ The curves were calculated using $\tilde{\epsilon}_a = -19.6 + i0.59$, $d = d_0 = 530 \text{ \AA}$, and $\epsilon_c = 2.25$.¹⁰ We note that in the ER configuration the value of k_{\parallel} of the incident and scattered radiation ranges from zero to $k_0 = \omega/c$, whereas in the ATR configuration the value of k_{\parallel} extends to $\epsilon_c^{1/2}k_0$.

The curves for the ER configuration are fairly flat. The maximum values of $|\epsilon_f\Gamma_{bzz}^E|^2$ and $|G_{fbzz}^E/\epsilon_f|^2 \cos\theta_s$, which occur at different values of k_{\parallel} (corresponding to $\theta_{i0} \sim 74^\circ$ and $\theta_{s0} \sim 52^\circ$, respectively), are 2.5 and 1.2, respectively. In the ATR configuration on the other hand the curves for $|\epsilon_f\Gamma_{cfzz}^P|^2 = |\Gamma_{cbzz}^{P_0}|^2$ and $|G_{fczz}^P/\epsilon_f|^2 \cos\theta_s = |G_{bczz}^{P_0}/\epsilon_f|^2 \cos\theta_s$ both exhibit very sharp peaks, at $k_{\parallel} = \epsilon_c^{1/2}k_0 \sin(\theta_P \simeq \theta_{\text{ATR}} = 43.6^\circ)$, having magni-

tudes of 250 and 4.0, respectively. (Both $|\Gamma_{cbzz}^{P_0}|^2$ and $|G_{bczz}^{P_0}/\epsilon_f|^2 \cos\theta_s$ fall to very small values when $k_{\parallel} \neq \epsilon_c^{1/2}k_0 \sin\theta_P$, i.e., when θ_i and θ_s differ from θ_P .) The enhancement of the (zz) scattering cross section of the overlayer resulting from the use of SEM waves is effectively $|G_{bc}^{P_0}\Gamma_{cb}^{P_0}|^2 \cos\theta_P / |G_{bf}^E\Gamma_{fb}^E|^2 \cos\theta_{s0} = 340$.

Since the magnitude of $|G_{fc}^P/\epsilon_f|^2 \cos\theta_P$ (~ 4.0) is not much greater than $|G_{fb}^E/\epsilon_f|^2 \cos\theta_{s0}$ (~ 1.2), one can still achieve an appreciable enhancement in the scattering cross section by using a mixed ATR prism-ER configuration¹¹ in which the incident radiation is a SEM wave and the scattered radiation is a VEM wave in the vacuum (medium b). The enhancement factor resulting from the use of this mixed configuration, $|\Gamma_{cf}^P(\theta_P)G_{fb}^E(\theta_{s0})|^2 / |\Gamma_{bf}^E(\theta_{i0})G_{fb}^E(\theta_{s0})|^2$, is approximately equal to 100. Recent measurement of Raman scattering by liquid benzene in a mixed ATR prism-ER scattering configuration, in which the benzene served as the surface inactive medium adjacent to the Ag film, indicated an enhancement in the scattering efficiency of $\simeq 75$.¹¹

The appreciable enhancement of the Γ_{cf}^P in the ATR prism configuration provides the possibility of using CAR scattering spectroscopy to obtain a further substantial increase in the Raman scattering intensities. In CAR scattering which is carried out using high-peak-power tunable laser sources, a fixed-frequency VEM wave at ω_1 interacts with a tunable VEM wave at ω_2 , via a third-order dielectric susceptibility, to generate a scattered VEM wave at $\omega_3 = 2\omega_1 - \omega_2$ and $\vec{k}_3 = 2\vec{k}_1 - \vec{k}_2$.³ The scattering exhibits a resonance when $\omega_1 - \omega_2 = \omega_R$ and $\vec{k}_1 - \vec{k}_2 = \vec{k}_R$, where ω_R and \vec{k}_R are the frequency and wave vector of the scattering modes. In using SEM waves in an ATR prism configuration, only the parallel components of the wave vector will be conserved. Furthermore, since the dispersion of $\partial k_{\parallel}/\partial\omega$ for the SEM waves is positive and relatively small, phase matching is possible at a small angle between the planes of incidence of the ω_1 and ω_2 SEM waves. The CAR scattering corresponds to four EM waves mixing with three incident waves and one scattered wave. The cross section for CAR scattering is therefore proportional to $|\Gamma(\omega_1)^2\Gamma(\omega_2)G(\omega_3)|^2 \times \cos\theta_s$. The use of SEM waves in CAR scattering at 6471 \AA by an overlayer on Ag surface would thus lead to an enhancement of the scattering intensity of the order of $\sim 10^6$ over that for VEM waves! The major limitation to CAR scattering in the ATR prism configuration is the need to limit the peak power of the laser sources to avoid

deterioration of the metal film.

Finally we note that our theoretical formulation is directly applicable to SEM-wave-enhanced light scattering by optical and acoustical phonons in metals.¹² It is also applicable, with only minor variation, to the SEM-wave-enhanced second-harmonic generation at an Ag-air interface which was recently investigated by Simon, Mitchell, and Watson¹³ using a Kretschmann prism configuration. With SEM waves as the incident radiation at the fundamental frequency ω_1 , wave-vector conservation [i.e., $\vec{k}_{\parallel}(\omega_2) = 2\vec{k}_{\parallel}(\omega_1)$] requires that the second-harmonic generated radiation at $\omega_2 = 2\omega_1$ in the metal film be transferred into the prism at an angle $\theta_s(\omega_2) = \sin^{-1} [k_{\parallel}(\omega_1)/k_0\epsilon_c^{1/2}]$ which differs appreciably from $\theta_P(\omega_2)$ because of the large dispersion between ω_1 and ω_2 . As a consequence the enhancement in the second-harmonic signal which results from the large value of $\Gamma_{cb}^{P_0}$ at $\theta_i(\omega_1) = \theta_P(\omega_1)$ is appreciably offset by the small values of $G_{bc}^{P_0}$ at $\theta_2(\omega_2)$ away from $\theta_P(\omega_2)$. This accounts in part for the apparent discrepancy between the observed enhancement and the estimate of the enhancement, which Simon, Mitchell, and Watson calculated solely on the basis of the enhancement of the electric fields at the metal-air interface alone.

We wish to acknowledge the valuable discussions with Dr. J. J. Wynn regarding CAR scattering.

*IBM Fellow (1975-1976).

†Work supported in part by the U. S. Army Research

Office, Durham, under Contract No. DAHC/0181 and by the Advanced Research Projects Agency under Contract No. CNF-44620-75-C-0069 (monitored by the U. S. Air Force Office of Scientific Research).

¹R. C. Greenler and T. L. Slager, *Spectrochim. Acta*, Part A **29**, 193 (1973).

²P. J. Hendra and E. J. Loader, *Trans. Faraday Soc.* **67**, 827 (1971).

³R. F. Begley, A. B. Harvey, and R. L. Byer, *Appl. Phys. Lett.* **25**, 387 (1974).

⁴E. Burstein, W. P. Chen, Y. J. Chen, and A. Hartstein, *J. Vac. Sci. Technol.* **11**, 1004 (1974).

⁵W. P. Chen, Y. J. Chen, and E. Burstein, to be published.

⁶A. Otto, in *Proceedings of the Taormina Conference on Polaritons*, edited by E. Burstein (Pergamon, New York, 1974), p. 117.

⁷J. Schoenwald, E. Burstein, and M. Elson, *Solid State Commun.* **12**, 185 (1973).

⁸D. L. Mills, A. A. Maradudin, and E. Burstein, *Ann. Phys. (N.Y.)* **56**, 504 (1970).

⁹The z components of the transfer functions are appreciably larger than the x components for both configurations. Moreover, the ratio of the x components and of the z components in the ER configuration to the corresponding components in the ATR prism configuration are roughly the same.

¹⁰*American Institute of Physics Handbook*, edited by D. E. Gray (McGraw-Hill, New York, 1972), 3rd ed., p. 149, Table 6G-1.

¹¹Y. J. Chen, W. P. Chen, and E. Burstein, *Bull. Am. Phys. Soc.* **21**, 338 (1976).

¹²Y. J. Chen, W. P. Chen, E. Burstein, and D. L. Mills, in *Proceedings of the International Conference on Light Scattering in Solids, Campinas, Brazil, 1975*, edited by M. Balkanski, R. C. C. Leite, and S. P. S. Porto (Flammarion, Paris, 1976), p. 525.

¹³H. J. Simon, D. E. Mitchell, and J. G. Watson, *Phys. Rev. Lett.* **27**, 1531 (1974).